HAL
open science

Viscosity and Morphology of Water-in-Water Emulsions: The Effect of Different Biopolymer Stabilizers

Lingsam Tea, Taco Nicolaï, Lazhar Benyahia, Frédéric F. Renou

To cite this version:

Lingsam Tea, Taco Nicolaï, Lazhar Benyahia, Frédéric F. Renou. Viscosity and Morphology of Water-in-Water Emulsions: The Effect of Different Biopolymer Stabilizers. Macromolecules, 2020, 53 (10), pp.3914-3922. 10.1021/acs.macromol.0c00204 . hal-03026664

HAL Id: hal-03026664
https://hal.science/hal-03026664v1

Submitted on 3 Dec 2020

HAL is a multi-disciplinary open access archive for the deposit and dissemination of scientific research documents, whether they are published or not. The documents may come from teaching and research institutions in France or abroad, or from public or private research centers.

L'archive ouverte pluridisciplinaire **HAL**, est destinée au dépôt et à la diffusion de documents scientifiques de niveau recherche, publiés ou non, émanant des établissements d'enseignement et de recherche français ou étrangers, des laboratoires publics ou privés.

Viscosity and morphology of water-in-water emulsions: the effect of different biopolymer stabilizers.

Lingsam Tea, Taco Nicolai, Lazhar, Benyahia, Frederic Renou*

Le Mans Université, IMMM UMR-CNRS 6283, 72085 Le Mans, cedex 9, France

for Table of Contents use only

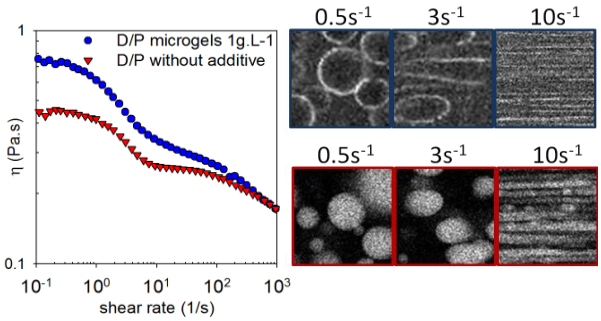

Abstract

Water-in-water (W/W) emulsions show a characteristic decrease of the viscosity with increasing shear rate that is well described by equations proposed in the literature. Confocal laser scanning microscopy images showed that the decrease of the viscosity was caused by deformation and alignment of the dispersed droplets followed by string formation. W/W emulsions stabilized by addition of polysaccharides or protein microgels still form strings when sheared with the particles remaining at the interface. After cessation of the flow the strings break up into small droplets and the presence of stabilizing particles inhibits their coalescence. It is shown how the viscosity and the microstructure depend on the initial droplet size, the interfacial tension, the viscosity of the two phases and the concentration of the stabilizing polymers.

KEYWORDS Emulsion; viscosity; aqueous two phase; mixture, structure; string

I. Introduction

Water-in-water (W/W) emulsions are formed by mixing two aqueous solutions of incompatible polymers[1]. Such emulsions are different from oil-in-water (O/W) emulsions in that their interfacial tension is orders of magnitude lower and their interface is broader. As a result, stabilization of W/W emulsions cannot be achieved by molecular surfactants. However, they can be stabilized by adding particles, which has received considerable attention in recent years, see for reviews ref. [2-4]. Recently, we reported that they can also in some cases be stabilized by linear polyelectrolytes[5]. The fact that stable W/W emulsions can be obtained opens the possibility to

use them for application in areas such as nutrition, cosmetics or pharmacy. It is therefore of interest to investigate their behavior under flow.

Taylor[6] was the first to propose an equation to describe the zero shear rate viscosity (η_0) of emulsions in general as a function of the volume fraction of the dispersed phase (ϕ) and the viscosity ratio (K) between that of the dispersed (η_d) and the continuous (η_c) phases:

$$\eta_0 = \eta_c \left[1 + \phi \frac{5K+2}{2K+2}\right] \tag{1}$$

This equation is valid only for dilute emulsions of incompressible liquids and does not include the effect of the shear rate ($\dot{\gamma}$), the radius of the droplets (R) or the interfacial tension (Γ). Under shear, the droplets can deform and align which leads to a reduction of the viscosity. These effects were taken into consideration by Kroy[7] (eq. 2) and by Frankel and Acrivos[8] (eq.3):

$$\eta = \frac{\eta_c}{1+(\tau\dot{\gamma})^2} \left[\frac{2K+2+3\Phi(K+0.4)}{2K+2-2\Phi(K+0.4)} + \frac{2K+3+3\Phi(K-1)}{2K+3-2\Phi(K-1)} \ (\tau\dot{\gamma})^2\right] \tag{2}$$

$$\eta = \frac{\eta_c}{1+(\tau\dot{\gamma})^2} \left[1 + \Phi \frac{5K+2}{2K+2} + \left(1 + \Phi \frac{5(K-1)}{2K+3}\right)(\tau\dot{\gamma})^2\right] \tag{3}$$

with

$$\tau = \frac{\eta_c R}{\Gamma} \frac{(19K+16)(2K+3-2\Phi(K-1))}{40(K+1)-8\Phi(5K+2)} \tag{4}$$

Here τ is the relaxation time of the droplets.

It is known that isolated droplets break above a critical shear rate that depends on the capillary number ($Ca = \eta_c \dot{\gamma} R/\Gamma$) and K[9]. However, studies on blends of incompatible synthetic polymers have shown that at higher dispersed volume fractions the deformed droplets align in the flow direction followed by rupture and coalescence to form strings above a critical shear rate that become thinner with increasing shear rate[10-13]. After cessation of the flow the strands quickly break up into small droplets due to Rayleigh instabilities.

W/W emulsions formed by mixing incompatible biopolymers have been much less investigated[14-17]. Capron *et al.*[15] investigated emulsions consisting of droplets of a phase rich in alginate dispersed in a continuous caseinate rich phase and vice versa. They found that the shear dependence of the viscosity could be well described by eq. 2. These authors did not study the morphology of the emulsions under shear and assumed that the dispersed droplets broke up above a critical shear rate. Wolf and Frith[17] studied the shear viscosity of W/W emulsions formed by mixtures of gelatin and dextran. They found that the viscosity at low shear rates and low volume fractions of the dispersed phase could be well described by an equation proposed by Choi and Schowalter[18], see eq.5, whereas the viscosity at high shear rates could be well described by a simple logarithmic mixing law over the whole range of volume fractions, see eq.6:

$$\eta = \eta_c \left[\frac{1+h_1 h_2 \dot{\gamma}^2}{1+h_2^2 \dot{\gamma}^2}\right] \qquad (5)$$

with

$$h_1 = \tau\left[1 + \Phi \frac{5(19K+16)}{4(K+1)(2K+3)}\right] \text{ and } h_2 = \tau\left[1 + \Phi \frac{3(19K+16)}{4(K+1)(2K+3)}\right]$$

$$\log(\eta_c) = \phi \log(\eta_d) + (1-\phi) \log(\eta_c) \qquad (6)$$

They observed that strings were formed above a critical shear rate that depended on the volume fraction and the viscosity ratio. The effect of shear on the morphology of W/W emulsions formed by the same biopolymer mixtures was investigated in more detail by Tromp and De Hoog[14]. These authors found that at a fixed shear rate the strings coalesce laterally with time into thicker strands and eventually form bands.

Here we present a more extensive and detailed investigation of the viscosity and the morphology of model W/W emulsions formed by mixtures of poly(ethylene oxide) (PEO) and dextran as a function of the shear rate. The shear rate dependence of the viscosity will be compared with the theoretical predictions mentioned above. The morphology was studied as a function of the shear rate utilizing confocal laser scanning microscopy (CLSM) combined with a specially designed shear device. The effect of the volume fraction and the interfacial tension was investigated. Furthermore, we compare the results obtained for unstable W/W emulsions with those obtained for W/W emulsions stabilized by the presence of different types of polysaccharides or by protein microgels. The effect of shear on the viscosity and morphology of stable W/W emulsions has not been reported before in the literature.

II. Materials and methods

Sample preparation

Dextran and PEO with weight average molar masses $M_w = 1.6 \times 10^5$ g.mol^{-1} and $M_w = 2 \times 10^5$ g.mol^{-1}, respectively, were purchased from Sigma-Aldrich. The powders were dissolved in

ultra-pure water (MilliQ). The PEO sample contained a very small amount of silica particles that were removed by centrifugation at $5x10^4$g for 4h30. Chitosan is a cationic polysaccharide with a pKa ≈ 6.5[19]. The chitosan sample used for this study was purchased from Sigma-Aldrich (batch STBG5137V) and had a degree of acetylation of 25% as determined by NMR. Diethyl aminoethyl dextran (DEAED) is a cationic polysaccharide obtained by functionalizing dextran with diethyl aminoethyl groups that are positively charged in a wide pH range (pKa≈9.5)[20]. The sample used for this study was purchased from Sigma-Aldrich and contained 80% functionalized sugar units. Stock solutions of chitosan and DEAED were prepared in MilliQ water by stirring overnight. κ-Carrageenan (KC) was purchased from Sigma-Aldrich. The weight average molar mass (M_w) and z-average hydrodynamic radii (R_h) were determined by light scattering techniques[5] yielding: M_w= 3.4×10^5 g/L and R_h = 58 nm for chitosan, M_w= $8x10^5$ g/mol and R_h = 39 nm for DEAED and M_w= $3.5x10^5$ g/mol and R_h = 60 nm for KC. Protein microgel particles were prepared by heating solutions at pH 6.1 of whey protein isolate (WPI) purchased from Lactalis (Laval, France) at a concentration of 40 g/L. R_h of the microgels was measured by dynamic light scattering as described elsewhere[21] and found to be 140 nm.

The emulsions were prepared by mixing the required amounts of each biopolymer solution using a vortex mixer. No effect of the mixing order or the mixing speed was seen on the morphology of the emulsions. We suggest that sufficient turbulent flow leads to complete homogeneous mixture of all components. Same results were obtained by dissolving the polymer in the PEO phase or dextran phase first. The pH was set to the desired values by addition of a small amount of NaOH (0.1M) or HCl (0.1M). The behavior of unstable emulsions, pure or in the presence of KC, was independent of the pH. Emulsions in the presence of protein microgels were stable at pH 7.0. Those in the presence of DEAED or chitosan were most stable at pH 5.0.

Interfacial tension

The interfacial tension of W/W emulsions is very low and is very difficult to determine accurately. Here we determined Γ at 20°C by analyzing the shape of the interface near a wall in terms of the capillary length (l_c)[22]:

$$\frac{x(z)}{l_c} = arccosh\left(\frac{2l_c}{z}\right) - arccosh\left(\frac{2l_c}{h}\right) - \sqrt{4 - \frac{z^2}{{l_c}^2}} + \sqrt{4 - \frac{h^2}{{l_c}^2}} \quad (7)$$

where x is the distance to a vertical wall, z is the height of the interface with respect to that far from the wall and h is the height at the wall. From the capillary length and the density difference between the two phases (Δρ) the interfacial tension can be calculated:

$$l_c = \sqrt{\frac{\Gamma}{\Delta\rho g}} \quad (8)$$

with g the gravitational constant. Δρ = 50 kg/mm^3 was measured within ±1 kg/mm with a Metler Toledo DM50 oscillating U-tube densimeter and was found within the experimental error to be the same with and without added polysaccharides The two phases were gently placed on top of each other in polystyrene cells after which the cells were centrifuged to remove air bubbles and to ensure full separation of the phases. The interface was imaged with a Nikon camera and the digitized interface was fitted to eq. 7, see figure S1 of the supplementary information.

Viscosity

146 Rheological measurements were done at 20°C with a stress-controlled rheometer (ARG2,
147 TA instruments) using a cone plate geometry (radius 40 mm, angle 2°). The emulsion was placed
148 in the geometry and presheared at 10^3 s^{-1} during 30 s, but longer preshear was found not to affect
149 the results. Subsequently, the viscosity was measured while decreasing the shear rate from 1000
150 s^{-1} to 0.01 s^{-1} and then increasing $\dot{\gamma}$ back to 1000 s^{-1}. We have applied fast shear rate ramps
151 taking only 2 min in order to avoid coalescence of the dispersed droplets, which is favored by
152 flow at low shear rates. At these conditions, the same viscosities were measured within 10%
153 when repeating shear ramps with the same sample or with different samples of the same
154 emulsion. The effect of the duration of the ramp is shown in Fig. S2a of the supplementary
155 information for unstabilized emulsions. No difference was found when the shear ramp took 1 or
156 2 min, but when the shear rate was increased more slowly the decrease of the viscosity started at
157 smaller $\dot{\gamma}$ and reached a higher plateau. Both at very low ($\dot{\gamma} < 0.1$ s^{-1}) and very high shear rates
158 the results were not significantly dependent on the duration of the shear ramp. The effect of the
159 duration of the shear rate ramp was weaker for emulsions in the presence of chitosan, see Fig.
160 S2b of the supplementary information, which might be expected as chitosan inhibited
161 coalescence. The temperature was controlled by a Peltier to within ±0.1°C.
162

163 **Confocal laser scanning microscopy**

164 Images were obtained with a Zeiss LSM800 CLSM microscope (Carl Zeiss Microscopy
165 GmbH, Germany) with two different objectives: HC×PL APO 10× (NA = 1.2) and a water
166 immersion HC×PL APO 25× (NA = 0.7). Images were taken at a rate of 3 frames per second. It
167 was shown elsewhere that the layer of chitosan or DEAED is very difficult to visualize using
168 labeled polysaccharides. However, the layer of labeled protein microgel could be easily

169 observed. Therefore, in most emulsions only the dextran phase was visualized by adding a small
170 amount of dextran labeled with FITC. In emulsions with protein microgels a small amount of
171 rhodamine B was added that binds spontaneously to the proteins. The droplets can nevertheless
172 still be observed because excess rhodamine B not bound to the microgels was not distributed
173 equally between the two phases. FITC was excited at 488 nm, whereas rhodamine B was excited
174 at 561 nm. The morphology of the emulsions under shear was visualized using a RheOptiCAD®
175 device (CAD Instruments, Les Essarts-le-Roi, France), consisting of two parallel plates
176 translating in opposite direction. The device can be used with different inversed microscopes and
177 was used here in combination with the CLSM microscope. For a detailed description of the
178 device see ref. [23]. The time during which the samples could be sheared depended on the gap and
179 the shear rate and was only a few seconds at the highest shear rates used here. The gap was set at
180 values between 500 μm and 200 μm and the emulsions were sheared at different rates between
181 0.5 and 120 s^{-1} after a preshear at 10 s^{-1} in order to start at each shear rate with approximately the
182 same droplet size distribution.
183
184 **III. Results and discussion**
185
186 In first instance, we investigated emulsions consisting of droplets of the PEO phase in a
187 continuous dextran phase (P/D) and vice versa (D/P). Emulsions with different volume fractions
188 of the dispersed phase were prepared at the same tie-line where phase separation was almost
189 complete with 161g/L dextran in one phase and 80.5g/L PEO in the other phase. The emulsions
190 where homogenized with a vortex mixer and immediately placed in the apparatus. Subsequently,
191 the emulsions were presheared at 10 s^{-1} during 5 s. Longer preshear did not affect the

morphology significantly. Figure 1 shows the morphology of the emulsions at rest immediately after being presheared at different phase volume fractions. The droplet size increased with increasing volume fraction of the dispersed phase and phase inversion is observed when the PEO phase volume fraction approached 50%.

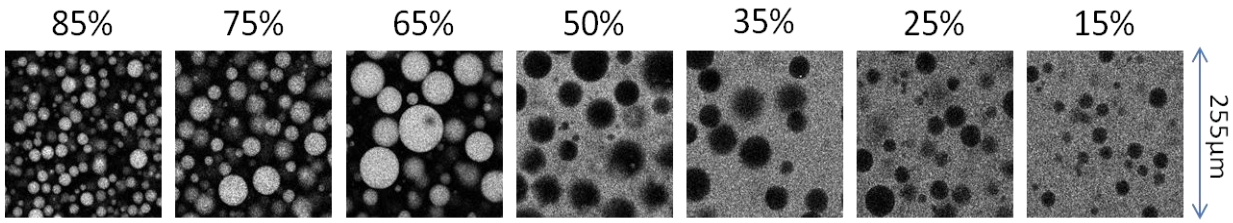

Figure 1. CLSM images obtained just after mixing of P-D emulsions at different PEO phase volume fractions indicated in the figure. The labeled dextran phase is indicated in white.

Viscosity

In figure 2 the viscosity is shown as a function of the shear rate for a P/D and a D/P emulsion at $\phi = 0.25$. The viscosity was found to decrease with increasing shear rate, but there was a distinct difference between results obtained during increasing and decreasing $\dot{\gamma}$. The same results were obtained when the shear rate ramps were repeated implying that there was no significant loss of material caused by shearing at high rates. Results obtained for the corresponding pure PEO and dextran phases are also shown in figure 2. The viscosity of the PEO phase was higher than that of the dextran phase and shows an effect of shear thinning for $\dot{\gamma} > 30$ s^{-1}. The comparison shows that η_0 was significantly larger for the emulsions than for the continuous phase. The effect of shear thinning was similar for the D/P emulsion and the pure PEO phase. Shear thinning for the P/D emulsion was much weaker than for the D/P emulsion, but it was stronger than that for the pure dextran phase. We may conclude that shear thinning of

212 the continuous phase is more important, but that shear thinning of the dispersed phase also
213 influences the viscosity of the emulsions.
214

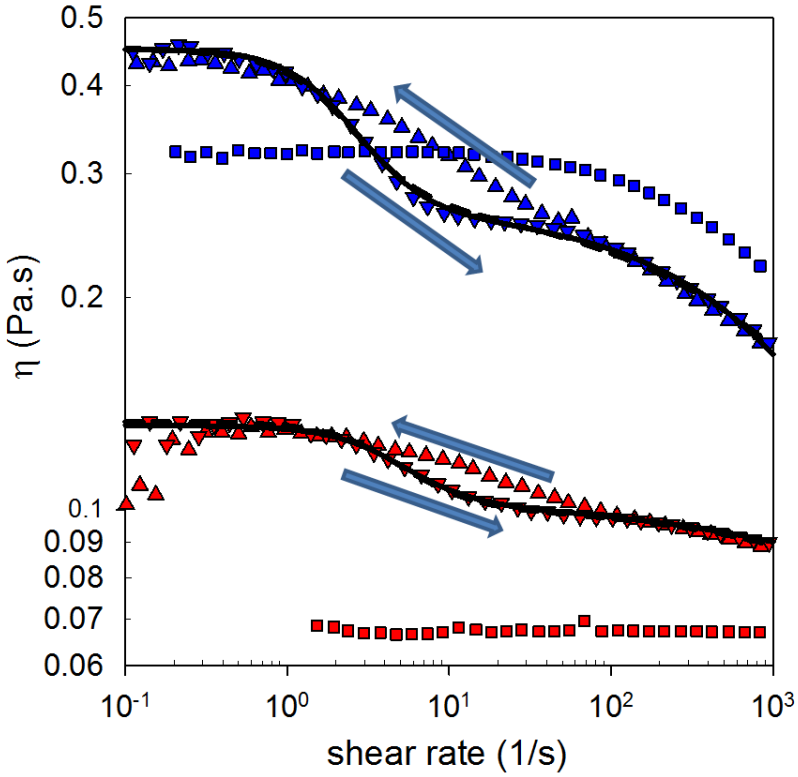

215

216 Figure 2. Viscosity as a function of the shear rate for emulsions of dextran in PEO (D/P) (blue
217 triangles) and PEO in dextran (P/D) (red triangles) at $\phi = 0.25$. The total duration of the shear
218 rate ramp was 2 min. For comparison the viscosities of the pure PEO (blue squares) and dextran
219 (red squares) phases are included. The solid and dashed lines represent fits of η during increasing
220 shear rate to eqs 2 and 3, respectively.

221

222 Figure 3 shows the viscosity as a function of increasing shear rate for emulsions at
223 different phase volume fractions. At all volume fractions hysteresis similar to that shown in

figure 2 was observed for decreasing shear rate, which was not shown in figure 3 for clarity. The zero-shear viscosity (η_0) increased with increasing volume fraction of the more viscous PEO phase (ϕ_{PEO}) until it reached a maximum at approximately 75% and then decreased to that of the pure PEO phase, see figure 4. The high shear rate viscosity (η_∞) was determined at approximately 20 s^{-1}, i.e. at the high frequency plateau where the effect of shear thinning was still negligible. η_∞ was found to increase progressively with increasing ϕ_{PEO}, see figure 4.

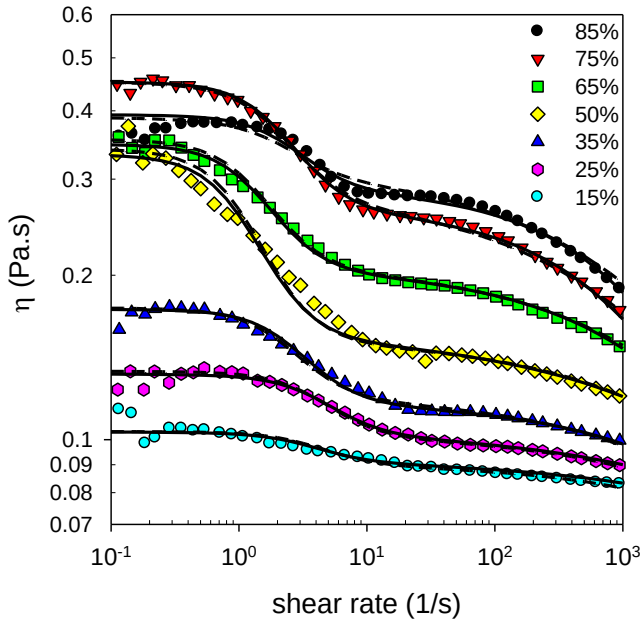

Figure 3. Viscosity as a function of increasing shear rate for P-D emulsions at different volume fractions of the PEO phase as indicated in the figure. The solid and dashed lines represent fits to eqs 2 and 3, respectively.

The dependence of η_0 and η_∞ on ϕ_{PEO} is compared in figure 4 with that calculated using eqs 2 and 3, which describe the data reasonably well at low volume fractions of the dispersed phase. The values of η_0 calculated using eq. 3 are equal to those proposed by Taylor (eq.1). Choi

238 and Schowalter[18] also proposed an equation for η_0 as a function of the volume fraction (see eq.5),
239 but the predicted values were much larger than the experimental data even at low volume
240 fractions of the dispersed phase. A similar discrepancy was reported for the W/W emulsions
241 studied by Kroy et al. However, Wolf and Frith[17] reported that the viscosity at low shear rate was
242 well described by the eq. 5 for dispersed volume fractions lower than 20%. The high shear rate
243 viscosities were also reasonably well described by eqs 2 and 3 at low dispersed volume fractions,
244 but a simple logarithmic mixing rule (eq.5) describes the data somewhat better over the whole
245 range of volume fractions. This was also the case for the W/W emulsions studied by Wolf et
246 Frith[17]. It is perhaps not surprising that the results at high shear rates do not correspond to the
247 theoretical predictions, because, as we will show below, strands are formed, which is not
248 considered in the theory. The discrepancy of η_0 at larger dispersed volume fractions shows that
249 the effect of interaction between the dispersed droplets was not correctly considered in the
250 theory.

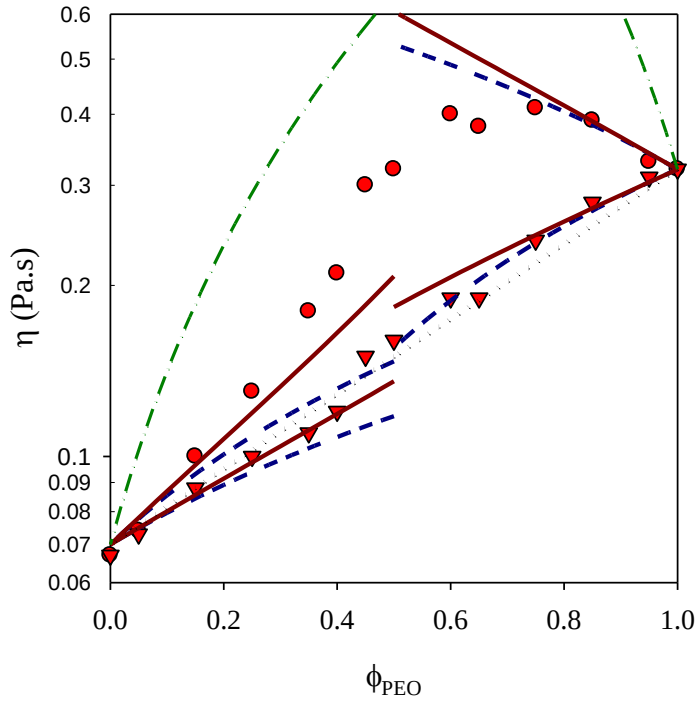

Figure 4. High (circle) and low (triangle) plateau viscosities as a function of the volume fraction of the PEO phase. The solid, dashed and dashed-dotted lines indicate theoretical predictions given by eqs 2, 3 and 5, respectively. The dotted line represents a logarithmic mixing rule (eq. 5).

The shear rate dependent viscosity was compared to the theoretical predictions given by eqs 2 and 3, see solid and dashed lines in figures 2 and 3. It was found that both equations well described the viscosity with increasing shear rate, but not with decreasing shear rate. In fact, the fit results obtained by eqs 2 and 3 practically overlap. Only for emulsions with equal phase volumes was the decrease of η with increasing shear rate more gradual than predicted by eqs 2 and 3. We note that it was necessary to include the effect of shear thinning on the viscosity of the PEO phase in order to fit the data at high shear rates. It appears that the three fit parameters of eqs 2 and 3 (η_c, η_d and τ) are enough to describe the viscosity well as a function of increasing

shear rate in spite of the fact that the theory does not consider strand formation at high shear rates. The real test of the theory is whether the values obtained from the fits are physically realistic.

In most cases there was little difference between the values of η_c, η_d and τ obtained from fits to eq 2 or eq 3, see figure 5. η_c was close to that of the pure PEO for $\phi_{PEO} > 75\%$ and close to that of the dextran phase for $\phi_{PEO} \leq 25\%$, see figure 5a. At intermediate volume fractions, η_c was intermediate between that of the pure phases. We believe that the agreement at $\phi_{PEO} = 50\%$ between η_c obtained from a fit to eq. 2 and the viscosity of the pure dextran phase is fortuitous. The values of η_d obtained from fits were in all cases intermediate between that of the pure PEO and dextran phases. The fit values of τ increased with increasing volume fraction of the dispersed phase, but at a given dispersed volume fraction τ was smaller for P/D emulsions ($\phi_{PEO} \leq 50\%$) than for D/P emulsions ($\phi_{PEO} \geq 60\%$).

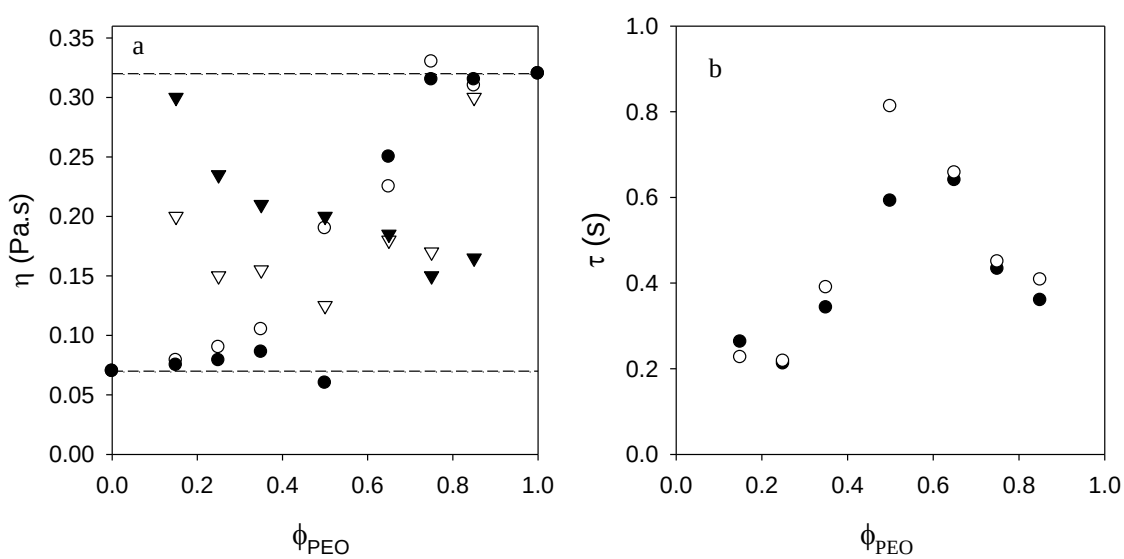

Figure 5. Viscosity of the continuous (η_c, circles) and dispersed (η_d, triangles) phases (a) and the relaxation time (b) obtained from fits to eq. 2 (filled symbols) and eq. 3 (open symbols). The

279 dashed lines in figure 5a indicate the viscosities of the pure PEO (upper line) and dextran (lower
280 line) phases.

281

282 The relaxation time obtained from the viscosity measurements is related to the zero-shear
283 viscosity of the two phases, the interfacial tension and the radius of the droplets, see eq. 4. The
284 emulsions at different volume fractions were prepared at the same tie-line, which means that
285 only the radius of the droplets varies. The larger τ at $\phi = 35\%$ corresponds to larger droplet sizes
286 seen with CLSM, see fig. 1. However, the values of R calculated from τ using the measured
287 interfacial tension ($\Gamma = 55 \pm 5\ \mu N.m^{-1}$) were larger (34 - 55 μm) than the volume averaged radii
288 derived from the CLSM images (9 - 27 μm). We conclude that there is a significant discrepancy
289 between the values of η_c, η_d and R derived from fits to eqs 2 or 3 and the real values determined
290 independently. Clearly, the theoretical equations developed so far do not correctly describe the
291 viscosity of W/W emulsions during shear flow and new models need to be developed that take
292 into consideration that the droplets strongly deform, orient and coalesce into strings.

293

294 **Morphology**

295 Figure 6 shows CLSM images of D/P and P/D emulsions that were taken while shearing
296 at different shear rates. A video of an emulsion during shear flow in real time is added as
297 supporting information. With increasing shear rate the droplets become more deformed and align
298 themselves in the flow. As the shear rate is increased further strings were formed. These results
299 are similar to those reported for other W/W emulsions reported in the literature[14, 17]. The
300 characteristic string morphology was reached within 1 s after the start of the measurement and
301 remained the same for the duration of the experiment. Unfortunately, the device used here does

not allow long durations of continuous shear. Therefore, we were not able to investigate the long time evolution of the microstructure with time under shear, which was shown by De Hoog and Tromp [14] to evolve slowly involving formation of thicker strands and eventually bands.

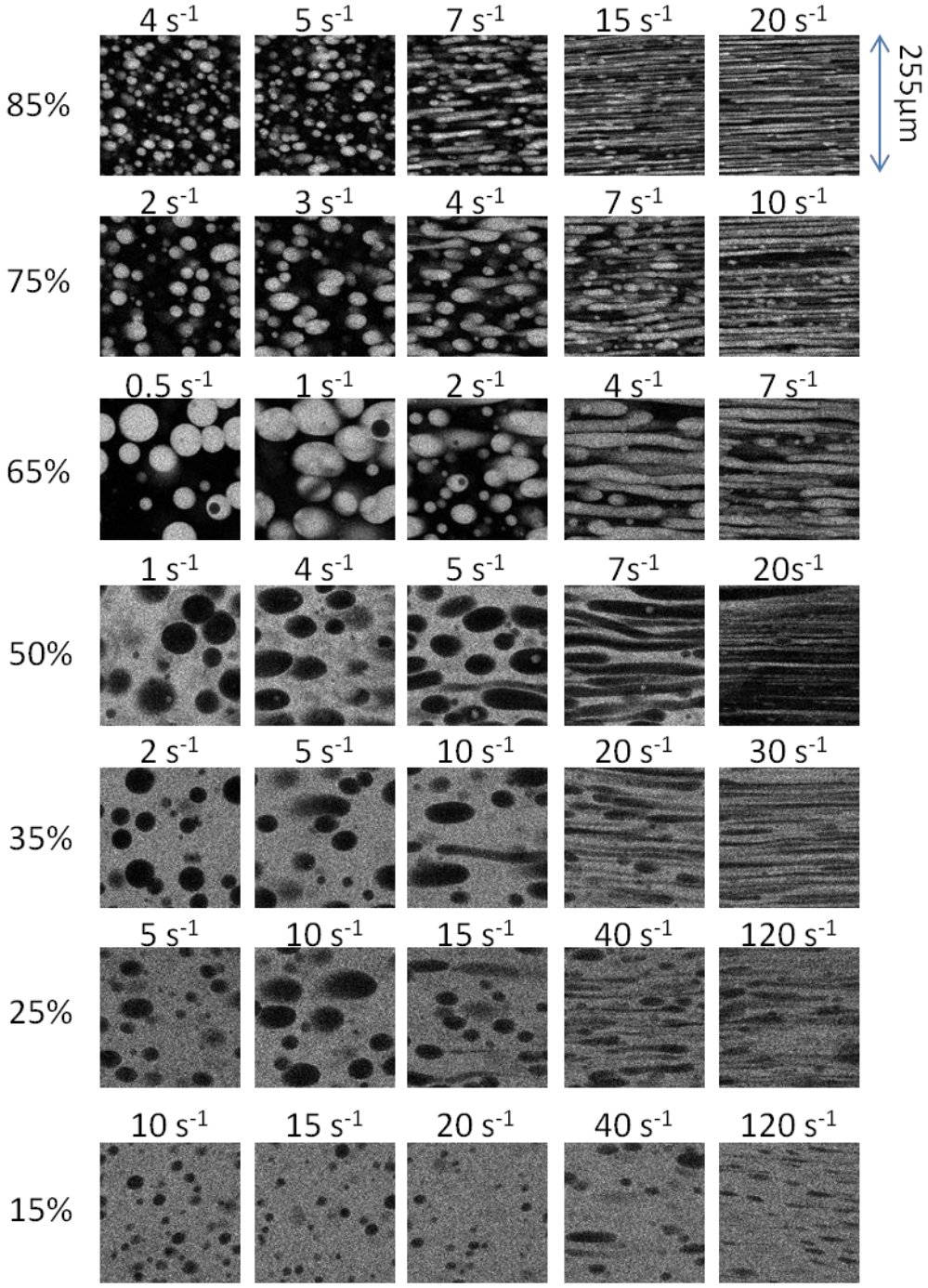

307 Figure 6. CLSM images of emulsions at different phase volume fractions at different shear rates
308 as indicated in the figure. The labeled dextran phase is indicated in white.

309

310 With increasing volume fraction of the dispersed phase, the shear rate at which the
311 droplets started to deform decreased, because the droplets at rest were larger. The shear rate at
312 which strings were formed also decreased with increasing ϕ, indicating that string formation is
313 easier at higher volume fractions. Droplet deformation and string formation started at higher
314 shear rates for P/D than for D/P emulsions at the same ϕ and droplet size, because it is easier to
315 deform droplets that are less viscous than the continuous phase. Comparison with the shear rate
316 dependent viscosity (figure 3) shows that the shear rate at which the droplets started to deform
317 corresponds approximately with the shear rate at which η started to decrease. The shear rate at
318 which most droplets were transformed into strings was significantly higher and corresponds
319 approximately to the shear rate at which the second plateau of the viscosity was reached. This
320 correspondence was also noted by Wolf and Frith[17]. They also observed an increase of the
321 critical shear rate with decreasing ϕ that was more important when the dispersed phase was more
322 viscous than the continuous phase.

323 Figure 7 shows CLSM images after cessation of the flow. It took approximately one
324 second to arrest all movement. A video is provided as supplementary information. With
325 decreasing shear rate the strands show Rayleigh instabilities and break-up into smaller strands
326 that subsequently contract and become spherical. After cessation of the flow, rapid coalescence
327 occurred between small droplets until approximately the same droplets size distribution as was
328 obtained as before application of the shear. However, since these emulsions were not stabilized,
329 coalescence continued to proceed slowly. We found that this latter process was faster when a low

shear rate was applied, presumably, because it favored collision between droplets. It is clear that the effect of increasing shear rate on the morphology is different from the effect of decreasing shear rate, which explains the hysteresis of the viscosity as a function of the shear rate.

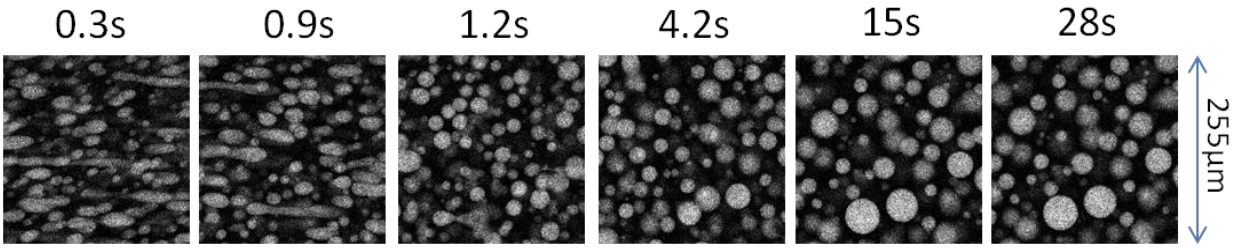

Figure 7. CLSM Images of a D/P emulsions ϕ=25% at different times after cessation of the flow at a shear rate of $10s^{-1}$ as indicated in the figure.

Effect of dilution

D/P emulsions at ϕ = 25% were diluted with water. Dextran droplets could still be seen in CLSM images after dilution by a factor 3, but when the emulsions were diluted by a factor 4 they became homogeneous. The volume fractions of the two phases remained the same for dilutions down to a factor two, but ϕ was smaller after dilution by a factor 3 (ϕ = 18%). Figure 8 shows the shear rate dependence of the viscosity at different dilutions. As expected, dilution caused a decrease of the viscosity and the interfacial tension and shifted the effect of shear thinning to higher shear rates. The decrease of the viscosity due to droplet deformation and alignment was observed at approximately the same shear rates down to dilution by a factor 3, but the effect of hysteresis became smaller and was negligible at dilution x3. Good fits to eq. 2 were obtained with τ = 0.33 s^{-1} and 0.34 s^{-1} for, respectively, dilutions x1.5 and x2.0, see solid lines in fig. 8. The data at dilution x3 were not good enough to obtained a reliable fit.

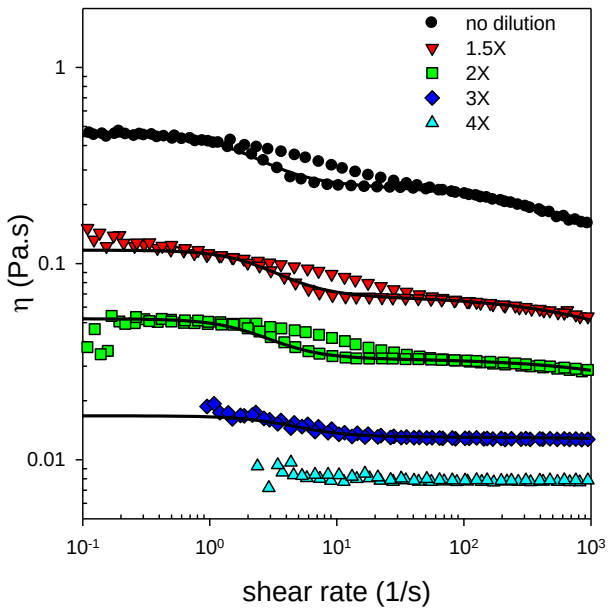

Figure 8. Viscosity as a function of increasing shear rate for D/P emulsions with ϕ = 25% at different dilutions indicated in the figure. The lines represent fits to eq. 2.

The effect of shear on the morphology did not depend much on the dilution down to x2, see figure 9. The droplet size before shear appeared slightly smaller after dilution by a factor 2 and the onset of droplet deformation and formation of strands started at slightly lower shear rates. The shear rate at which emulsion droplets start to deform depends on R, K, Γ and η_c, see eq. 4, but the effect of dilution on R and K, which decreases to K = 2.5 at dilution x3, was small compared to the effect on Γ and η_c which both decreased strongly upon dilution. We found Γ = 16±2μN.m^{-1}, η_c = 0.09 Pa.s at dilution x1.5 and 6±2μN.m^{-1}, η_c = 0.04 Pa.s at dilution x2. Using measured values of K, Γ and η_c, we obtained R = 30 μm and 23 μm at dilution x1.5 and x2. It appears therefore that, by chance, the decrease of the viscosity is compensated by the decrease of

363 the interfacial tension, which explains why the shear rate dependence of the viscosity and the
364 morphology was not much influenced by dilution.

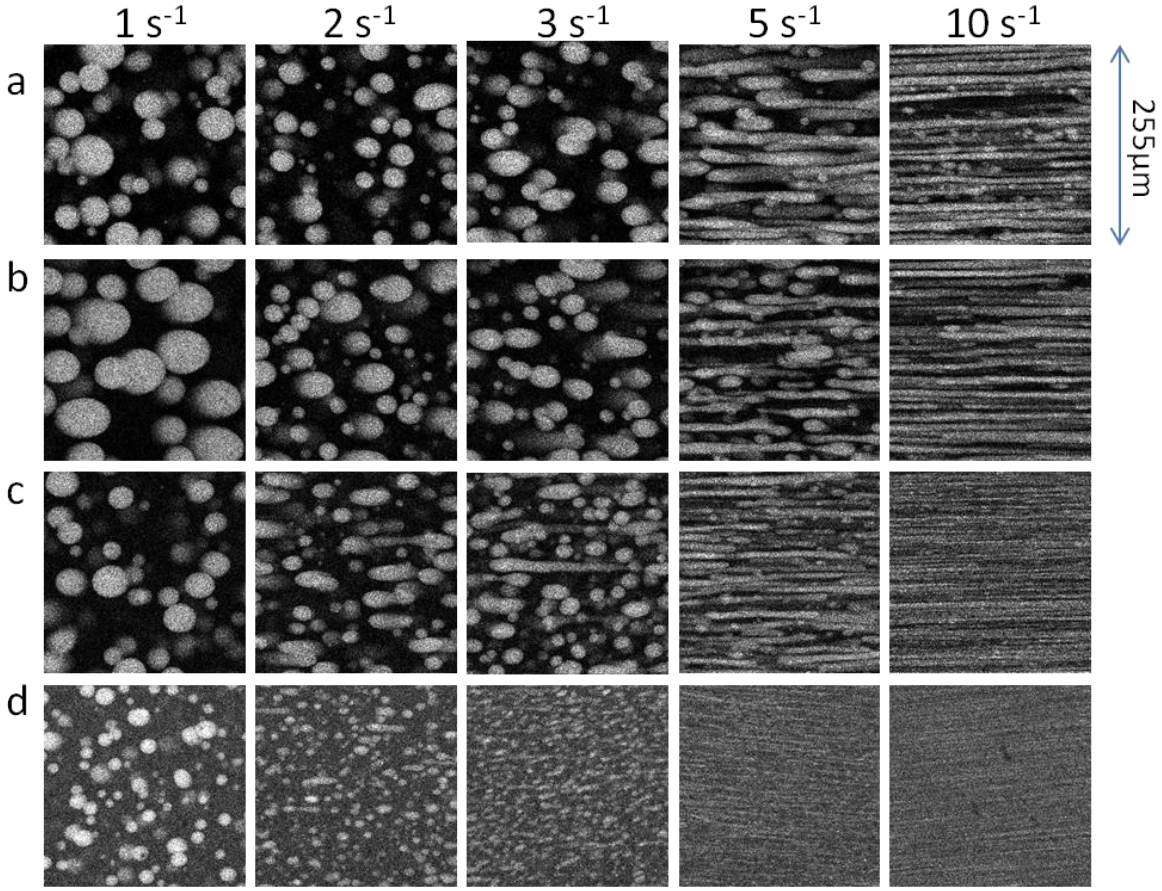

365

366 Figure 9. CLSM images of D/P emulsions at ϕ = 25% at different dilutions factors and shear
367 rates. The dilution factors were from top to bottom: x1(a), x1.5(b), x2(c) and x3(d).

368

369 **Emulsions stabilized by polysaccharides**

370

371 D/P emulsions at pH 5 can be stabilized for at least a week by addition of chitosan or
372 DEAED[5]. Interestingly, we found in this study that there was no influence of adding
373 polysaccharides on the interfacial tension within the experimental error. In figure 10 we show the

effect of adding 1g.L^{-1} of chitosan or DEAED on the shear rate dependence of the viscosity of D/P emulsions with ϕ = 25%. The principal effect of adding these polysaccharides was an increase of the viscosity and stronger shear thinning at high shear rates. For comparison, we also show the effect of adding 1 g/L κ-carrageenan (KC), which is a polysaccharides that does not stabilize D/P emulsions. KC had a similar effect on the viscosity as DEAED. CLSM images using fluorescently labeled polysaccharides showed that the majority of the added polymers was distributed between the two phases with only a small amount situated at the interface[5]. The shear rate dependence of the viscosity could be well described by eq. 2 with τ = 0.31 , 0.37 and 0.82 s^{-1}, for chitosan, DEAED and KC, respectively, see solid lines in fig. 10. The values of η_c obtained from the fits were compatible with that of the pure PEO phase containing the amount of added polysaccharide that partitioned to the PEO phase. We note that the viscosity of the polysaccharides in pure water at 1 g/L was less than 10^{-2} Pa.s.

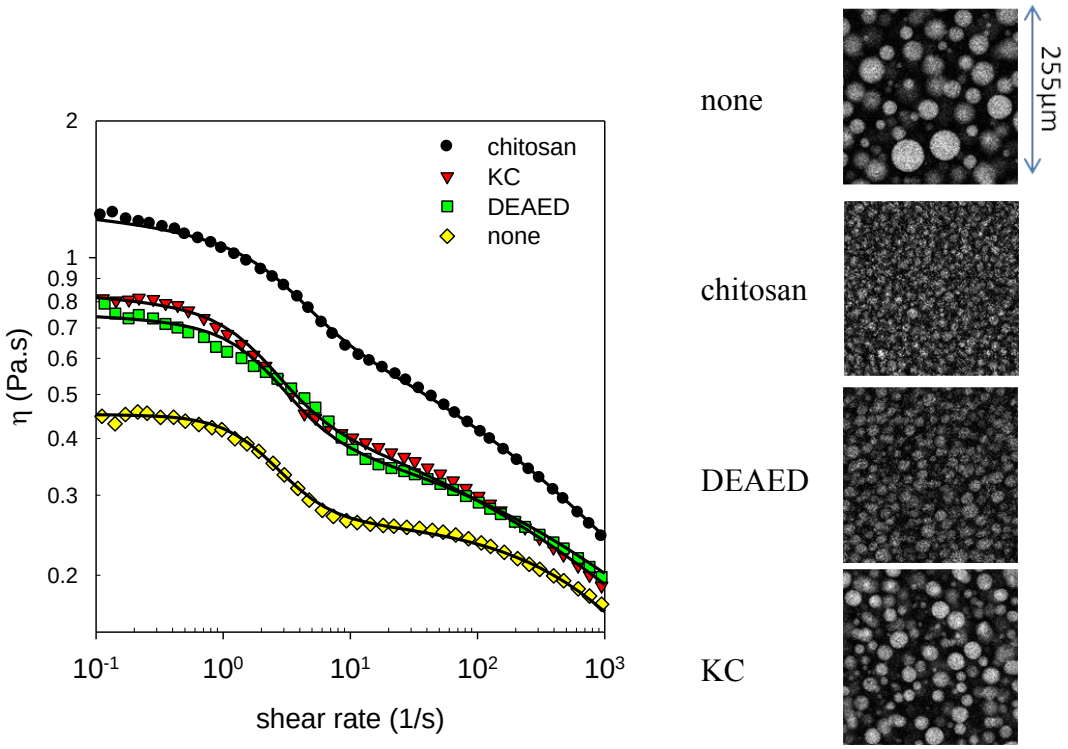

Figure 10. Viscosity as a function of increasing shear rate for D/P emulsions with ϕ = 25% with or without 1 g/L of different added polysaccharides as indicated in the figure. The lines represent fits to eq. 2. CLSM images of the emulsions just after cessation of shear at 10 s^{-1} are also shown.

CLSM images of the emulsions obtained just after shearing are shown in fig. 10. It is clear that addition of stabilizing polysaccharides has an effect on the droplet size as was already discussed elsewhere[5]. We suggest that the initial rapid coalescence is interrupted when a layer around the droplet is formed that is sufficiently dense and coherent. The size of the droplets immediately after shearing depends therefore on the rate at which the stabilizing layer is formed and not just on the volume fraction of the dispersed phase and the viscosity of the continuous phase. It appears that this process was for these emulsions faste for chitosan than for DEAED

leading to smaller droplets for emulsions containing the former. The rate of subsequent slow coalescence is hugely decreased by the presence of the stabilizing layer.

The effect of adding 1 g/L of the polysaccharides was also studied at other phase volume fractions, see figures S3 and S4 of the supplementary information. Qualitatively, the effect of the phase volume fractions was similar to that of emulsions without added polymers shown in figures 3 and 5. There are, of course, quantitative differences caused by the higher viscosities of the phases and the smaller droplet size.

The effect of adding polysaccharides on the morphology at different shear rates is shown in fig. 11. In all cases strings were formed under high shear. It is clear that the layer of chitosan and DEAED is not strong enough to resist the shear flow even though it does inhibit coalescence at rest. The droplets just after cessation of shear at 10 s^{-1} were significantly smaller in the presence of chitosan and DEAED. In the presence of KC the droplets were also smaller than for pure D/P emulsions, but larger than in the presence of chitosan or DEAED. The droplets started to align and deform at slightly higher shear rates in the presence of chitosan and DEAED than in the presence of KC. The small effect of chitosan or DEAED on τ can be explained by a compensation of the increase of the viscosity by the decreases of the droplet size as there was no measurable effect on Γ. Another important observation is that applying a low shear rate led to more rapid coalescence in the presence of non-stabilizing KC, but not in the presence of stabilizing chitosan and DEAED.

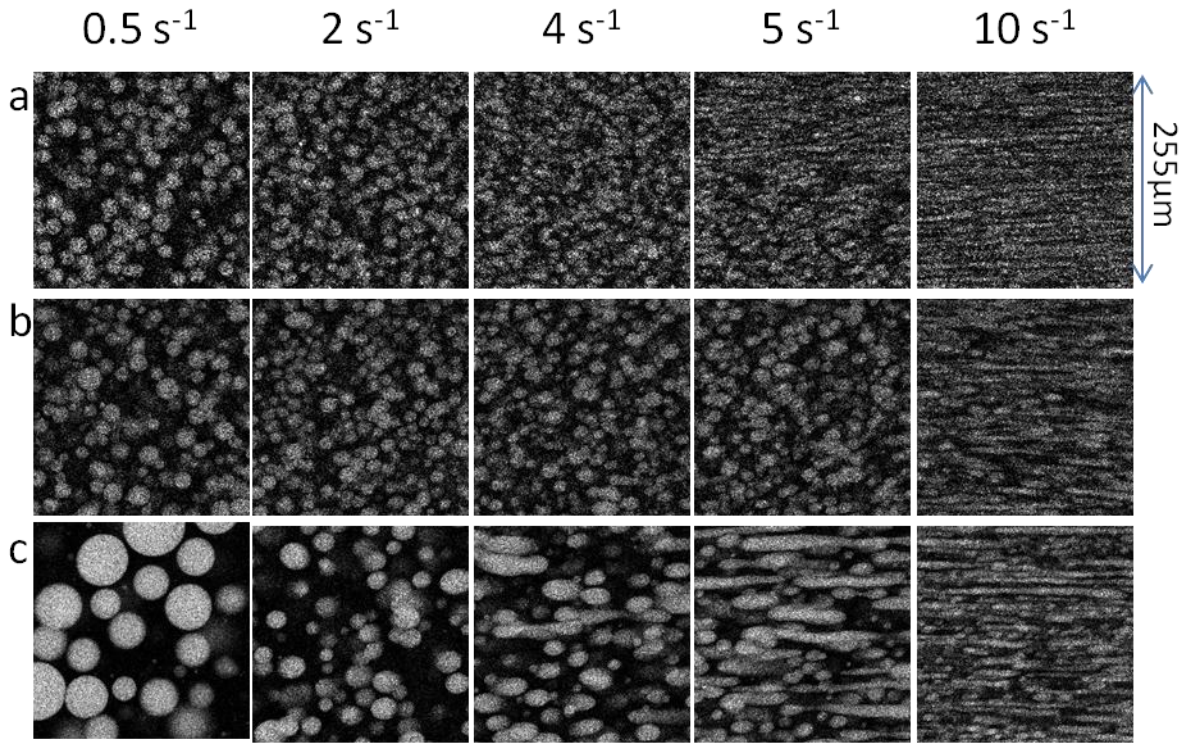

Figure 11. CLSM images of D/P emulsions containing 1 g/L chitosan (a), DEAED (b) or KC(c) at different shear rates.

Results obtained with smaller amounts of added polysaccharide were intermediate between those without addition and at 1 g/L, see figures S5 and S6 of the supplementary information. As might be expected, the viscosity and the effect of shear thinning decreased with decreasing chitosan concentration. But τ obtained from fits to eq. 2 did not depend strongly on the added polysaccharide concentration. CLSM measurements showed that decreasing the chitosan concentration caused an increase of the droplet size after cessation of the shear at 10 s^{-1}, see figure S5. However, there was not a strong effect of the chitosan concentration on the shear rate at which droplet deformation and strand formation started in agreement with the weak variation of τ. The small effect of the added polysaccharide concentration can again be explained

432 by a compensation between the decrease of the viscosity and the decrease of the droplet size. We
433 may therefore conclude that the effect of adding a stabilizing polymer is principally to inhibit
434 coalescence, but that behaviour of stable and unstable W/W emulsions under shear flow is
435 qualitatively the same.
436
437 **Emulsions stabilized by protein microgels**
438 An important question is whether the particles remain at the interface during shearing and
439 in particular during string formation. The density of the chitosan and DEAED at the interface is
440 low so that it is difficult to visualize the adsorbed layer with CLSM. Therefore, we repeated a
441 few measurements with emulsions in the presence of protein microgels with a radius of about
442 140 nm. A detailed investigation of the effect of adding protein microgels on the stability of
443 these W/W emulsions has been reported elsewhere [24]. It was found that the microgels accumulate
444 at the interface both for D/P and P/D emulsions, but that P/D emulsions were more stable than
445 D/P emulsions.
446 The shear rate dependence of the viscosity was similar to that observed for pure
447 emulsions or in the presence of polysaccharides, see fig. S8 of the supplementary information.
448 Fig. 12 shows CLSM images of D/P and P/D emulsions at ϕ = 25% containing 1 g/L protein
449 microgels. A video is provided as supplementary information. The layer of adsorbed labeled
450 microgels can be clearly seen surrounding the dispersed droplets. We note that excess
451 fluorophore that was not attached to the proteins partitioned preferentially to the PEO phase.
452 With increasing shear, droplet deformation and string formation were observed similar to
453 emulsions in the presence of polysaccharides and started at a higher critical shear rate for the P/D
454 emulsion compared to the D/P emulsion. It is clear from the images that the particles remained

455 adsorbed at the interface even at high shear rates when the strings were very thin. We may
456 assume that the same was the case for the adsorbed chitosan and DEAED.

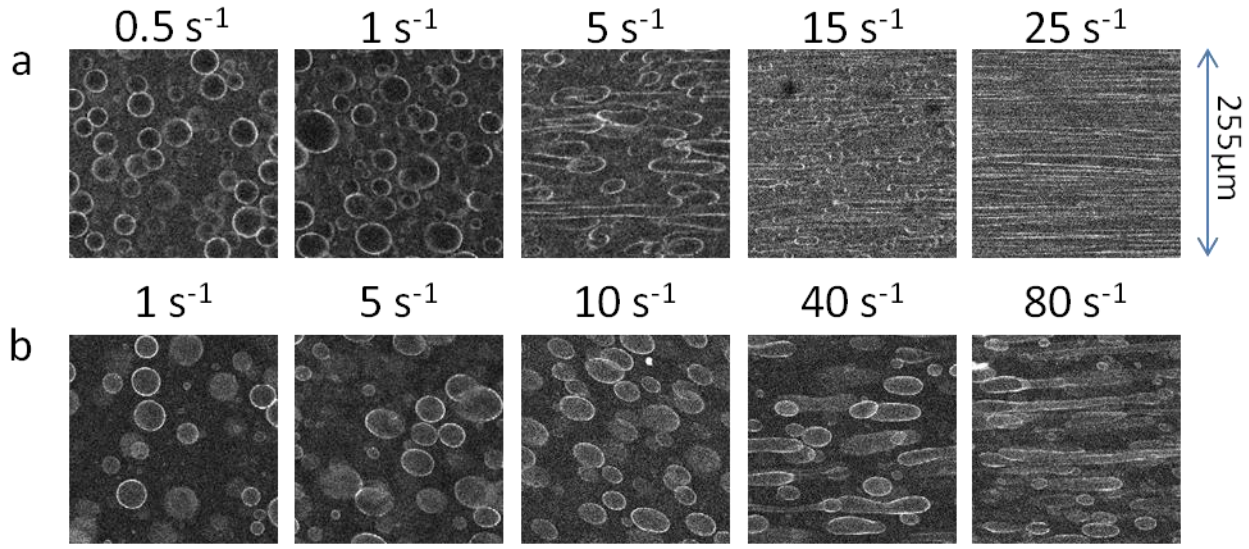

457

458 Figure 12. CLSM images of D/P (a) and P/D (b) emulsions containing 1 g/L of labeled protein
459 microgels at different shear rates. The volume fraction of the dispersed phase was 25%.

460

461 Fig. 13 shows the evolution of the morphology of a D/P emulsion after cessation of the
462 flow at a shear rate of 10^{-1}. The strings rapidly broke up into small droplets that were surrounded
463 by a layer of microgels. Rapid relaxation of deformed droplets and limited coalescence was
464 again observed just after cessation of the flow, but steady state was reached quickly. P/D
465 emulsions remained stable in this state for a period of at least a week, but coalescence continued
466 slowly for D/P emulsions.

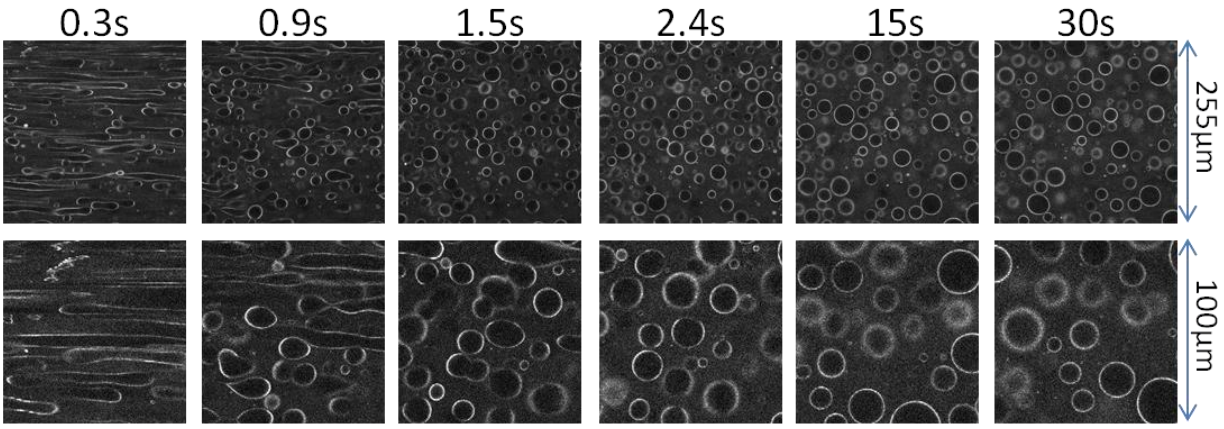

Figure 13. CLSM images at two different scales of D/P emulsions containing 1 g/L whey protein at different times after cessation of the flow at a rate of $10s^{-1}$ indicated in the figure.

Emulsions with the same viscosity for the dispersed and continuous phase.

In this study we have investigated emulsions for which the dispersed phase was either four times more or four times less viscous that the continuous phase. One might wonder whether the difference between in viscosity is important for the behavior of these emulsions under shear even though the equations that were proposed to describe the behavior do not have particular features at K=1. Therefore we prepared W/W emulsions with η=0.08 Pa.s for both phases. by choosing a PEO with a lower molar mass ($M_w = 1 \times 10^5$ g.mol^{-1}). Results for emulsions with and without protein microgels showed the same qualitative features both for unstable emulsions and emulsions in the presence of protein microgels, see figures S9-11 of the supplementary information. Strings were still formed with the microgels remaining at the interface. The conclusion is that the general features of the behavior of W/W emulsions under shear presented here do not require a significant difference in the viscosity of the two phases.

IV. Conclusion

The viscosity of W/W emulsions decreases at a characteristic shear rate due to deformation and alignment of dispersed droplets. At higher shear rates a process of rupture and coalesce leads to the formation of strands that become thinner with increasing shear rate. During cessation of the flow the strands break up into small droplets that rapidly coalesce to form larger droplets and then continue to coalesce slowly. Flow at a low shear rate favors this later stage of slow coalescence.

The dependence of the viscosity with increasing shear rate can be well described by equations proposed in the literature if the effect of shear thinning of the two phases is taken into consideration. However, the dependence of the viscosity during decreasing shear rate is different and cannot be described by these equations. At fixed intermediate shear rates the viscosity increased slowly implying that the emulsions evolve with time and that steady state was not reached during the shear rate ramps. The characteristic shear rates where the droplets start to deform and where strings are formed depend on the initial droplet size, the interfacial tension and the viscosities of the two phases.

When the W/W emulsions are stabilized by adding certain types of polysaccharides or protein microgels, strand formation is still observed and the behavior under shear flow is not significantly modified by the layer at the interface formed by these particles. However, coalescence of the droplets formed by break-up of the strands after cessation of the shear is inhibited. Particles adsorbed at the interface remain at the interface even when fine strings are formed under strong shear. The small droplets formed immediately after cessation of flow already contain a surface layer of adsorbed particles.

508 **Supporting Information**.

509 -Effect of the duration of the shear rate ramp on the dependence of the viscosity of W/W
510 emulsions on the shear rate.

511 -The effect of the phase volume fractions on the shear rate dependence of the viscosity for
512 emulsions in the presence of 1 g/L polysaccharide.

513 -Dependence on ϕ_{PEO} of η_c , η_d, and τ for emulsions in the presence of $1 g.L^{-1}$ polysaccharide.

514 -Viscosity as a function of the shear rate for D/P emulsions with ϕ_{PEO} = 25% in the presence of
515 different concentrations of polysaccharide and CLSM images of the emulsions taken shortly after
516 cessation of the shear at $10\ s^{-1}$.

517 - Viscosity of continuous phase and radii of droplets of different systems obtained from fits to
518 eq. 2.

519 - CLSM images obtained at different shear rates for D/P emulsions at ϕ=25% in the presence of
520 different concentrations of chitosan.

521 - Viscosity as a function of the shear rate for emulsions at ϕ = 0.25 containing 1 g/L protein
522 microgels.

523 - CLSM video of a dextran in PEO emulsions during and after shear at $10s^{-1}$. (Video 1)

524 - CLSM video of a dextran in PEO emulsions containing 1 g/L protein microgels during and
525 after shear at $10s^{-1}$. (Video 2)

526 -Behaviour under shear of W/W emulsions with the same viscosity for the dispersed and
527 continuous phase.

528

529

530 AUTHOR INFORMATION

531 Corresponding Author

532 Taco Nicolai: Taco.Nicolai@univ-lemans.fr.

533 References

534 1. Frith, W. J. Mixed biopolymer aqueous solutions–phase behaviour and rheology.
535 *Advances in Colloid and Interface Science* **2010,** 161 (1-2), 48-60.

2. Esquena, J. Water-in-water (W/W) emulsions. *Current Opinion in Colloid & Interface Science* **2016,** 25, 109-119.
3. Nicolai, T.; Murray, B. Particle stabilized water in water emulsions. *Food Hydrocolloids* **2017,** 68, 157-163.
4. Dickinson, E. Particle-based stabilization of water-in-water emulsions containing mixed biopolymers. *Trends in Food Science & Technology* **2018**, 83, 31-40.
5. Tea, L.; Nicolai, T.; Renou, F. Stabilization of Water-in-Water Emulsions by Linear Homo-Polyelectrolytes. *Langmuir* **2019**, 35, 9029−9036.
6. Taylor, G. I. The viscosity of a fluid containing small drops of another fluid. *Proceedings of the Royal Society of London. Series A, Containing Papers of a Mathematical and Physical Character* **1932,** 138 (834), 41-48.
7. Kroy, K.; Capron, I.; Djabourov, M. On the Viscosity of Emulsions. *arXiv preprint physics/9911078* **1999**.
8. Frankel, N.; Acrivos, A. The constitutive equation for a dilute emulsion. *Journal of Fluid Mechanics* **1970,** 44 (1), 65-78.
9. Grace, H. P. Dispersion phenomena in high viscosity immiscible fluid systems and application of static mixers as dispersion devices in such systems. *Chemical Engineering Communications* **1982,** 14 (3-6), 225-277.
10. Hashimoto, T.; Matsuzaka, K.; Moses, E.; Onuki, A. String phase in phase-separating fluids under shear flow. *Physical review letters* **1995,** 74 (1), 126.
11. Jeon, H.; Hobbie, E. K. Shear viscosity of phase-separating polymer blends with viscous asymmetry. *Physical Review E* **2001,** 63 (6), 061403.
12. Kim, S.; Hobbie, E. K.; Yu, J.-W.; Han, C. C. Droplet breakup and shear-induced mixing in critical polymer blends. *Macromolecules* **1997,** 30 (26), 8245-8253.
13. Migler, K. B. String formation in sheared polymer blends: Coalescence, breakup, and finite size effects. *Physical review letters* **2001,** 86 (6), 1023.
14. Tromp, R. H.; De Hoog, E. H. Band formation on shearing in phase-separated polymer solutions. *Physical Review E* **2008,** 77 (3), 031503.
15. Capron, I.; Costeux, S.; Djabourov, M. Water in water emulsions: phase separation and rheology of biopolymer solutions. *Rheologica Acta* **2001,** 40 (5), 441-456.
16. Wolf, B.; Frith, W. J.; Singleton, S.; Tassieri, M.; Norton, I. T. Shear behaviour of biopolymer suspensions with spheroidal and cylindrical particles. *Rheologica Acta* **2001,** 40 (3), 238-247.
17. Wolf, B.; Frith, W. J. String phase formation in biopolymer aqueous solution blends. *Journal of Rheology* **2003,** 47 (5), 1151-1170.
18. Choi, S. J.; Schowalter, W. Rheological properties of nondilute suspensions of deformable particles. *The Physics of Fluids* **1975,** 18 (4), 420-427.
19. Ahmed, K. F.; Aschi, A.; Nicolai, T. Formation and characterization of chitosan-protein particles with fractal whey protein aggregates. *Colloids and Surfaces B: Biointerfaces* **2018,** 169, 257-264.
20. Heinze, T.; Liebert, T.; Heublein, B.; Hornig, S., Functional polymers based on dextran. In *Polysaccharides Ii*, Springer: 2006; pp 199-291.
21. Phan-Xuan, T.; Durand, D.; Nicolai, T.; Donato, L.; Schmitt, C.; Bovetto, L. On the crucial importance of the pH for the formation and self-stabilization of protein microgels and strands. *Langmuir* **2011,** 27 (24), 15092-15101.

581 22. Tromp, R.; Blokhuis, E. Tension, rigidity, and preferential curvature of interfaces
582 between coexisting polymer solutions. *Macromolecules* **2013,** 46 (9), 3639-3647.
583 23. Boitte, J.-B.; Vizcaino, C.; Benyahia, L.; Herry, J.-M.; Michon, C.; Hayert, M. In *A novel*
584 *rheo-optical device for studying food complex systems under controlled double plate shear*,
585 Review of Scientific Instruments **2013**, 84, 013709 (2013).
586 24. Nguyen, B. T.; Nicolai, T.; Benyahia, L. Stabilization of water-in-water emulsions by
587 addition of protein particles. *Langmuir* **2013,** 29 (34), 10658-10664.
588
589